Supplement of

Analysis of inorganic chlorine chemistry in the midlatitude summer stratosphere using aircraft and satellite observations

David M. Wilmouth[1], Jennifer S. Hare[1], Laila V. Howar[2], Ross J. Salawitch[2], Eric J. Hintsa[3,4], Jessica B. Smith[1], David S. Sayres[1], James G. Anderson[1], Jason M. St. Clair[5,6], Erin R. Delaria[2,5], Reem A. Hannun[7], Thomas F. Hanisco[5], Daniel J. Czizco[8,9], Xiaoli Shen[8,10], Cameron R. Homeyer[11], Michelle L. Santee[12], T. Paul Bui[7,13], Paul A. Newman[5,6], Frank N. Keutsch[1], and Kenneth P. Bowman[14]

[1]Harvard University, Cambridge, MA, USA; [2]University of Maryland, College Park, MD, USA; [3]Cooperative Institute for Research in Environmental Sciences, University of Colorado Boulder, Boulder, CO, USA; [4]NOAA Global Monitoring Laboratory, Boulder, CO, USA; [5]NASA Goddard Space Flight Center, Greenbelt, MD, USA; [6]University of Maryland, Baltimore County, Baltimore, MD, USA; [7]NASA Ames Research Center, Moffett Field, CA, USA; [8]Purdue University, West Lafayette, IN, USA; [9]University of Chicago, Chicago, IL, USA; [10]Institute of Meteorology and Climate Research, Karlsruhe Institute of Technology, Eggenstein-Leopoldshafen, Germany; [11]University of Oklahoma, Norman, OK, USA; [12]Jet Propulsion Laboratory, California Institute of Technology, Pasadena, CA, USA; [13]Bay Area Environmental Research Institute, Moffett Field, CA, USA; [14]Texas A&M University, College Station, TX, USA

Correspondence: David M. Wilmouth (wilmouth@huarp.harvard.edu)

This file includes:
Text S1
Figures S1 – S5
References

Text S1. Harvard Halogens (HAL) flight instrument

The Halogens flight instrument from Harvard has participated in NASA collaborative aircraft missions for decades, dating back to 1987 when its ClO measurements over the Antarctic vortex provided the first quantitative link between ClO and O_3 destruction, i.e., the so-called 'smoking gun' linking CFC-derived chlorine to the ozone hole (Anderson et al., 1989a). Previous versions of the flight instrument provided the first aircraft measurements of ClO and BrO in the stratosphere (e.g., Brune et al., 1988a/b; Anderson et al.,1989a/b; Brune et al., 1989a/b; Toohey et al., 1990; Anderson et al., 1991), the first in situ aircraft measurements of $ClONO_2$ (Stimpfle et al., 1999), and the first measurements of ClOOCl in the atmosphere (Stimpfle et al., 2004; Wilmouth et al., 2006). The instrument has undergone 4 major redesigns and rebuilds since its first flight in 1987 and several name changes.

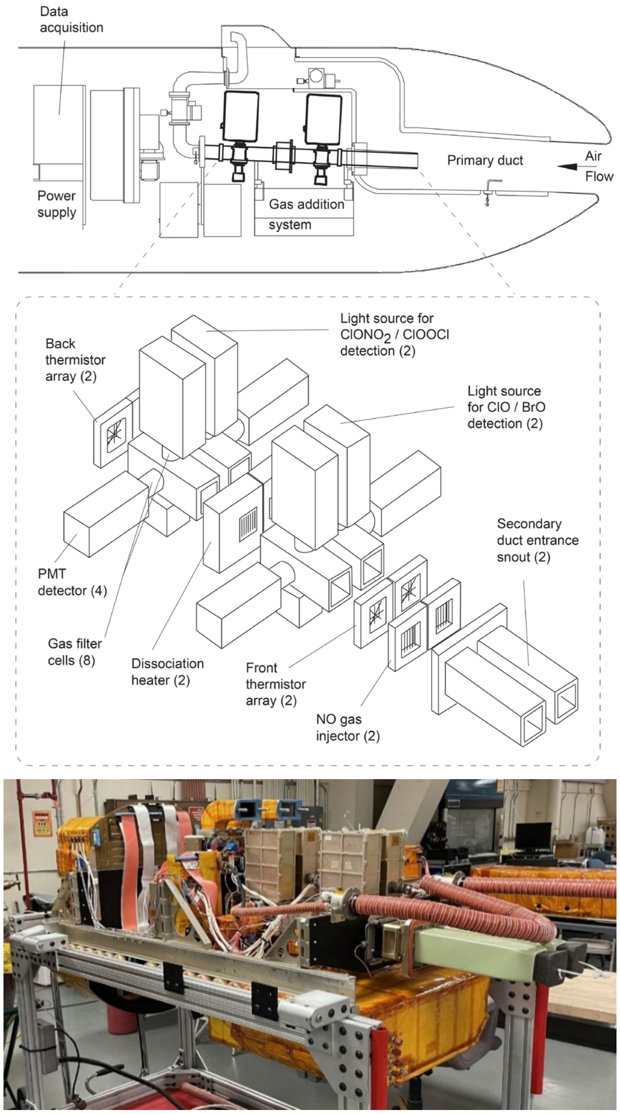

Figure S1. Cross-sectional view of the Harvard Halogens (HAL) flight instrument in an aircraft superpod with a close-up of the critical elements and a pre-flight instrument photo taken from the hangar lab space during the NASA DCOTSS mission.

Work on the present version of the instrument, now called the Harvard Halogens (HAL) flight instrument as flown in DCOTSS, began in 2019. ClO and $ClONO_2$ were measured by HAL from the left superpod of the ER-2 throughout both years of the DCOTSS campaign. The instrument exhibited excellent performance during the DCOTSS mission, successfully operating on all 29 research flights.

As shown in Figure S1, the flow of ambient air through the instrument is controlled by a single primary bypass duct, 20-cm diameter, and twin nested secondary ducts, 5-cm square. The laminar core of the primary flow is extracted and decelerated to ~10–15 m/s into the two mirror-image secondary ducts, where the ClO, $ClONO_2$, ClOOCl, and BrO measurements are made. For DCOTSS, the targeted measurements were ClO and $ClONO_2$, thus the instrument discussion here focuses only on those two measurements. The nested-duct design not only aids in slowing the sample air but also in maintaining laminar flow and minimizing wall contact. The entrance to each secondary duct is a 26-cm long fairing.

Just aft of the secondary duct inlets, nitric oxide injectors, consisting of nine perforated teflon tubes, mix dilute NO (1:5 NO in N_2 along with nitrogen carrier gas) uniformly into the flow. An array of seven fast-response platinum resistance thermistors mounted on wire supports in each duct monitor the ambient air temperature immediately forward of the front detection axes, where Cl from the titration of ClO with NO is detected via ultraviolet resonance fluorescence. Each front detection axis is followed by a silicon strip dissociation heater, capable of reaching very high temperatures, while having inert surfaces that will not compromise the halogen measurements. The heaters are custom built in our laboratory. The heaters raise the air temperature to dissociate $ClONO_2$ prior to the rear detection axes, where dissociated ClO from $ClONO_2$ is titrated with NO, and the resulting Cl atoms are measured. A second thermistor assembly downstream of the rear axis in each duct provides temperature data for the heated flow and allows feedback control of the heater.

A pitot tube at the rear of the secondary duct reads ambient pressure and velocity, while a throttle valve near the secondary duct exit is used to control the flow velocity. Other components of the instrument include a gas deck, where NO and air for the gas filter cell purges are housed, a heater controller, flight computer, data acquisition system, and power supplies.

The fluorescence signals at the front detection axes are modulated primarily by the addition of NO, while the fluorescence signals at the rear detection axes are modulated by both NO addition and flow temperature. The typical mode of instrument operation involves a 35-second NO addition cycle consisting of four different flows followed by a null flow, where NO is off. The lowest two NO flow rates are chosen to optimize the conversion to Cl atoms for ClO, while the highest two flows optimize the conversion to Cl for $ClONO_2$. The NO addition cycle is synchronized with the dissociation heater control algorithm of longer duration, which cycles the temperature in each duct. The temperature needed to rapidly dissociate $ClONO_2$ in the duct is approximately 500 K.

While the normal operating configuration is as described above with ClO measured in the front axes and $ClONO_2$ measured in the rear, the twin duct design allows for considerable flexibility in choosing the number and location of detectors. By adjusting NO flows and operation of the dissociation heaters, the instrument can be configured for additional redundancy; for many flights during DCOTSS, ClO detection axes were positioned at three of the four locations with only a single $ClONO_2$ detection axis to maximize signal:noise for the ClO measurements.

The resonance fluorescence detection technique used by the HAL flight instrument utilizes custom-built resonance fluorescence lamps fabricated in our laboratory (Hare et al., 2024). Each lamp consists of a 14 mm diameter quartz tube adjoined by two sidearms and filled with low pressure (~4 torr) Helium. One sidearm of the lamp has platinum chloride, $PtCl_2$. This sidearm is heated to promote $PtCl_2$ thermal dissociation, thereby serving as a source of Cl_2 to the discharge. The other sidearm contains barium metal (Ba, generated from pyrolysis of barium azide, BaN_6), which serves as a getter for chlorine as well as impurities in the lamp. A plasma discharge is sustained in the lamp body using a 20 W, 180 MHz radio-frequency power supply. Upon entering the discharge, Cl_2 is dissociated into chlorine atoms, which are excited primarily via electron impact, and then fluoresce, emitting a photon. The emitted VUV radiation passes through the base of the lamp, which is fitted with a MgF_2 window, into the instrument flow tube. Chlorine atoms in the flow tube are excited by light from the chlorine lamp and fluoresce. Fluorescence is detected by a photomultiplier tube (PMT) positioned perpendicular to the lamp. Custom circuitry ensures stable lamp output, and gas filter cells positioned before the lamps and PMTs serve to isolate the Cl line at 118.9 nm. The only other significant spectral line output from each lamp is a Lyman-alpha impurity at 121.6 nm, but with our lamp conditioning process, the Lyman-alpha impact is small and can be corrected. The gas filter cells and flow tube section at the detection axes are baffled to optimize Rayleigh scattering with respect to chamber scatter. Painstaking optimization in the laboratory of the full optical system between the lamp and PMT is essential for achieving the best signal:noise ratio of the measurements in flight.

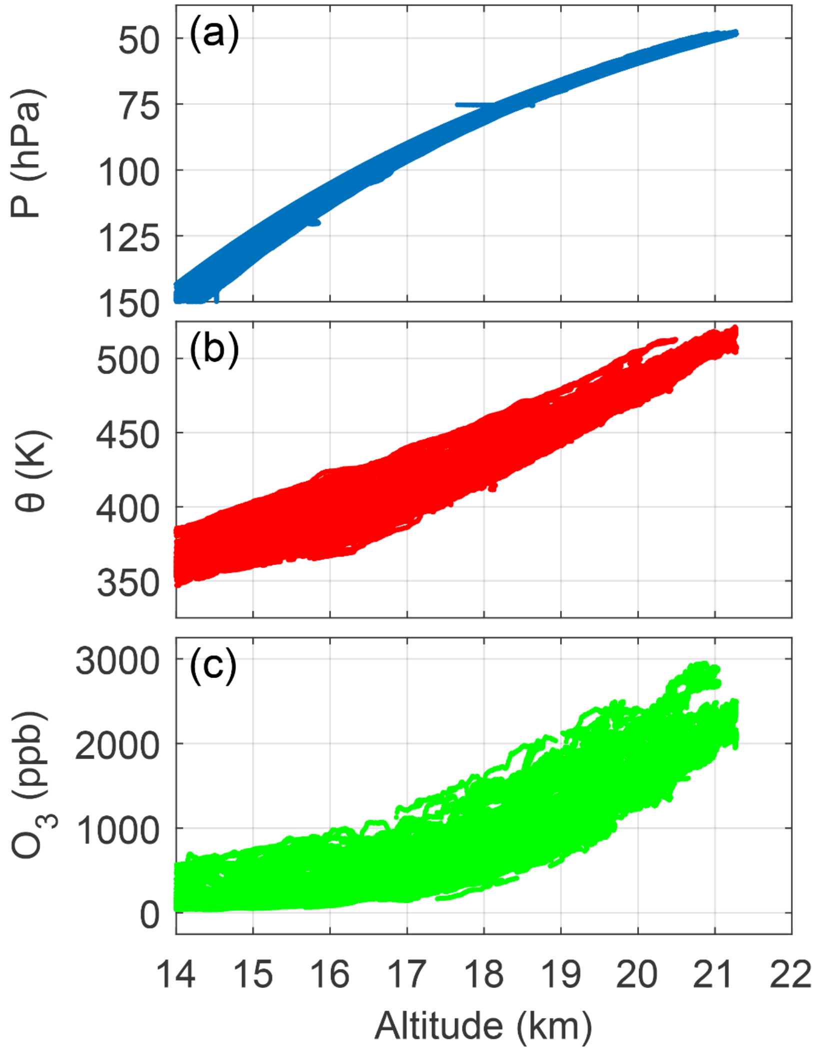

Figure S2. Comparison of vertical coordinate data as a function of altitude from all 29 research flights in the NASA DCOTSS mission: (a) pressure, (b) potential temperature, (c) ozone.

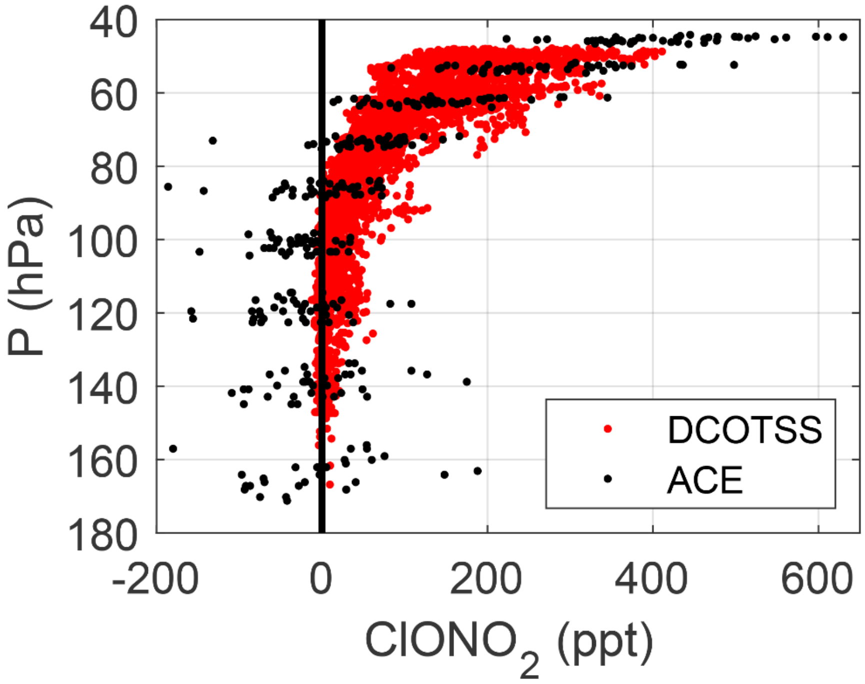

Figure S3. Comparison of $ClONO_2$ data as a function of pressure from the HAL instrument in DCOTSS and from the ACE satellite instrument. In situ data from DCOTSS are for all 29 research flights of the mission. $ClONO_2$ data from ACE were selected for the summers of 2021 and 2022 over the approximate contiguous U.S. (30 – 50˚ N latitude, 70 – 125˚ W longitude) and filtered for 3-sigma outliers per ACE recommendations (at altitudes <18.5 km). The vertical black line is plotted at 0 to more easily identify positive and negative values. The number of DCOTSS points shown is 5129, and the number of available ACE points is 360, as the satellite sampling over the US in summer is sparse.

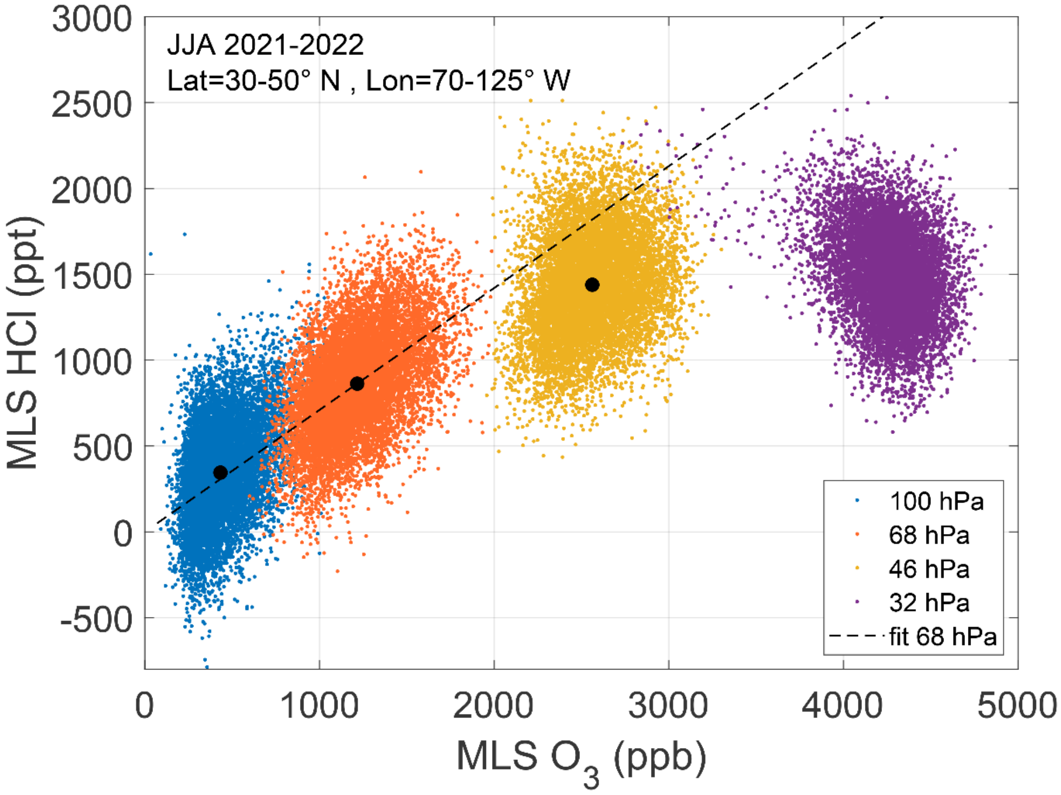

Figure S4. Scatter plot of HCl and O_3 measurements from the MLS satellite instrument obtained during the summers of 2021 and 2022 over the approximate contiguous U.S. (30 – 50° N latitude, 70 – 125° W longitude). Available data are shown for 4 MLS pressure levels: 100, 68, 46, and 32 hPa. Black dots represent the mean HCl and mean O_3 mixing ratios at each pressure level used in this study. The dashed black line is shown for reference and represents the 7.1×10^{-4} slope determined from the mean ratio at 68 hPa, as shown in Figure 6a. While the HCl:O_3 mean ratio at 100 hPa is close to that at 68 hPa, the relationship is different at 46 hPa and changes substantially by 32 hPa, as O_3 begins to rise much faster than HCl at the lower pressure levels. The total number of points plotted at each pressure level is 10,100. The MLS HCl data at 147 hPa have a high bias (Froidevaux et al., 2008; Livesey et al., 2022) and are not shown.

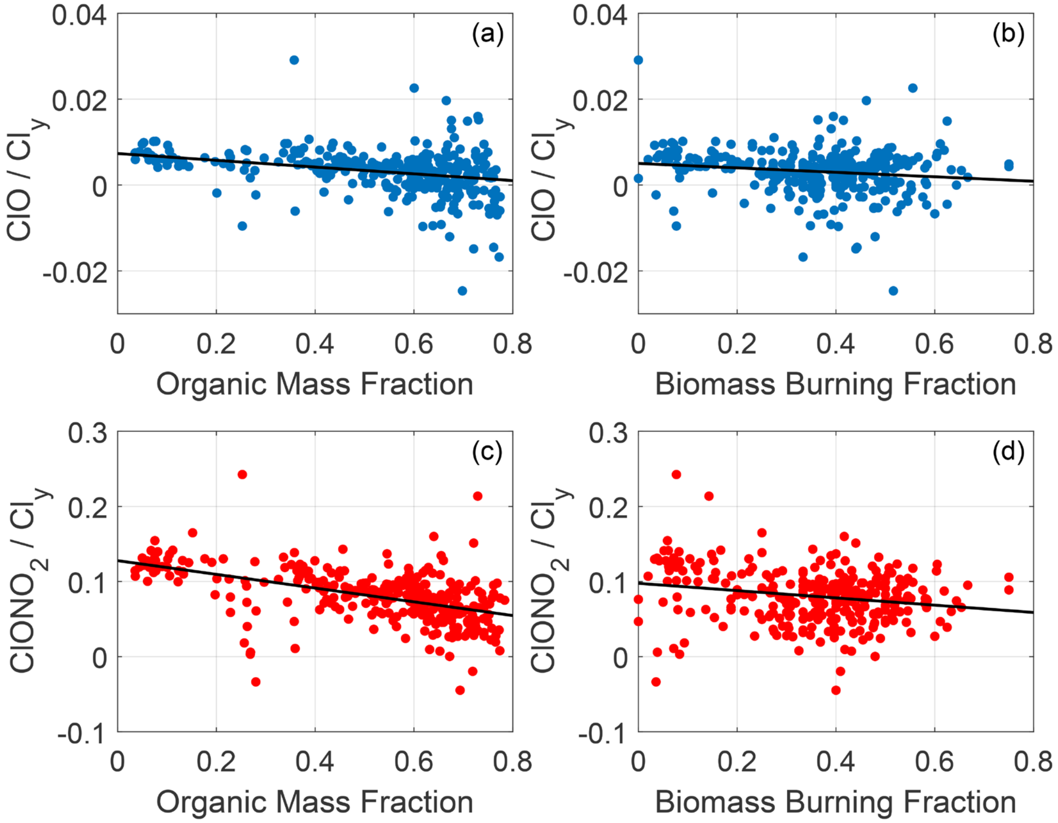

Figure S5. Inorganic chlorine partitioning in the stratosphere for (a), (b) ClO and (c), (d) $ClONO_2$ as function of organic mass fraction and biomass burning fraction (by particle number), respectively. Analogous plot to Figure 8 in the main text. Plotted are data from the 16 DCOTSS flights (all in 2022) where aerosol fractional values were reported; data shown are for potential temperature ≥ 390 K, and ClO measurements are only shown for solar zenith angle $\leq 75^\circ$. Due to the relatively sparse reporting of the aerosol fractional data, the inorganic chlorine data are interpolated to the fractional data; this introduces very little error. The black lines in each panel represent least-squares fits to the data.

References

Anderson, J. G., Brune, W. H., and Proffitt, M. H.: Ozone destruction by chlorine radicals within the Antarctic vortex: the spatial and temporal evolution of ClO-O_3 anticorrelation based on in situ ER-2 data, J. Geophys. Res., 94, 11465–11479, doi:10.1029/JD094iD09p11465, 1989a.

Anderson, J. G., Brune, W. H., Lloyd, S. A., Toohey, D. W., Sander, S. P., Starr, W. L., Loewenstein, M., and Podolske, J. R.: Kinetics of O_3 destruction by ClO and BrO within the Antarctic vortex: An analysis based on in situ ER-2 data, J. Geophys. Res., 94, 11480–11520, doi:10.1029/JD094iD09p11480, 1989b.

Anderson, J. G., Brune, W. H., and Toohey, D. W.: Free radicals within the Antarctic vortex: the role of CFCs in Antarctic ozone loss, Science, 251, 39–46, doi:10.1126/science.251.4989.39, 1991.

Brune, W. H., Toohey, D. W., Anderson, J. G., Starr, W. L., Vedder, J. F., and Danielson, E. F.: In situ northern mid-latitude observations of ClO, O_3, and BrO in the wintertime lower stratosphere, Science, 242, 558–562, doi:10.1126/science.242.4878.558, 1988a.

Brune, W. H., Weinstock, E. M., and Anderson, J. G.: Midlatitude ClO below 22 km altitude: measurements with a new aircraft-borne instrument, Geophys. Res. Lett., 15, 144–147, doi:10.1029/GL015i002p00144, 1988b.

Brune, W. H., Anderson, J. G., and Chan, K. R.: In situ observations of BrO over Antarctica: ER-2 aircraft results from 54°S to 72°S latitude, J. Geophys. Res., 94, 16639–16647, doi:10.1029/JD094iD14p16639, 1989a.

Brune, W. H., Anderson, J. G., and Chan, K. R.: In situ observations of ClO in the Antarctic: ER-2 aircraft results from 54°S to 72°S latitude, J. Geophys. Res., 94, 16649–16663, doi:10.1029/JD094iD14p16649, 1989b.

Froidevaux, L., Jiang, Y. B., Lambert, A., Livesey, N. J., Read, W. G., Waters, J. W., Fuller, R. A., Marcy, T. P., Popp, P. J., Gao, R. S., Fahey, D. W., Jucks, K. W., Stachnik, R. A., Toon, G. C., Christensen, L. E., Webster, C. R., Bernath, P. F., Boone, C. D., Walker, K. A., Pumphrey, H. C., Harwood, R. S., Manney, G. L., Schwartz, M. J., Daffer, W. H., Drouin, B. J., Cofield, R. E., Cuddy, D. T., Jarnot, R. F., Knosp, B. W., Perun, V. S., Snyder, W. V., Stek, P. C., Thurstans, R. P., and Wagner, P. A.: Validation of Aura Microwave Limb Sounder HCl measurements, J. Geophys. Res., 113, D15S25, doi:10.1029/2007JD009025, 2008.

Hare, J. S., Wilmouth, D. M., Smith, J. B., Klobas, J. E., Toohey, D. W., Hannun, R. A., Pittman, J. V., and Anderson, J. G.: Method for the production of a compact source of atomic line spectra in the vacuum ultraviolet, Appl. Optics, 63, 3685–3694, doi:10.1364/AO.520905, 2024.

Stimpfle, R. M., Cohen, R. C., Bonne, G. P., Voss, P. B., Perkins, K. K., Koch, L. C., Anderson, J. G., Salawitch, R. J., Lloyd, S. A., Gao, R. S., Del Negro, L. A., Keim, E. R., and Bui, T. P.: The coupling of $ClONO_2$, ClO, and NO_2 in the lower stratosphere from in situ observations using the NASA ER-2 aircraft, J. Geophys. Res., 104, 26705–26714, doi:/10.1029/1999JD900288, 1999.

Stimpfle, R. M., Wilmouth, D. M., Salawitch, R. J., and Anderson, J. G.: First measurements of ClOOCl in the stratosphere: the coupling of ClOOCl and ClO in the Arctic polar vortex, J. Geophys. Res., 109, D03301, doi:10.1029/2003JD003811, 2004.

Toohey, D. W., Anderson, J. G., Brune, W. H., and Chan, K. R.: In situ measurements of BrO in the Arctic stratosphere, Geophys. Res. Lett., 17, 513–516, doi:10.1029/GL017i004p00513, 1990.

Wilmouth, D. M., Stimpfle, R. M., Anderson, J. G., Elkins, J. W., Hurst, D. F., Salawitch, R. J., and Lait, L. R.: Evolution of inorganic chlorine partitioning in the Arctic polar vortex, J. Geophys. Res., 111, D16308, doi:10.1029/2005JD006951, 2006.